https://doi.org/10.5194/acp-2020-983
Preprint. Discussion started: 12 October 2020


Atmospheric Chemistry and Physics Discussions

# Heterogeneous Interactions between $SO_2$ and Organic Peroxides in Submicron Aerosol

Shunyao Wang[1], Tengyu Liu[2], Jinmyung Jang[1],

Jonathan P.D. Abbatt[2] and Arthur W.H. Chan[1*]

[1] Department of Chemical Engineering and Applied Chemistry, University of Toronto, Toronto, Ontario, M5S 3E5, Canada

[2] Department of Chemistry, University of Toronto, Toronto, Ontario, M5S 3H6, Canada

*Correspondence to: Arthur W.H. Chan (arthurwh.chan@utoronto.ca)

https://doi.org/10.5194/acp-2020-983
Preprint. Discussion started: 12 October 2020


Atmospheric Chemistry and Physics Discussions


## Abstract

Atmospheric models often underestimate particulate sulfate, a major component in ambient aerosol, suggesting missing sulfate formation mechanisms in the models. Heterogeneous reactions between $SO_2$ and aerosol play an important role in particulate sulfate formation and its physicochemical evolution. Here we study the reactive uptake kinetics of $SO_2$ onto aerosol containing organic peroxides. We present chamber studies of $SO_2$ reactive uptake performed under different relative humidities (RH), particulate peroxide contents, peroxide types, and aerosol acidities. Using different model organic peroxides mixed with ammonium sulfate particles, $SO_2$ uptake coefficient ($\gamma_{SO2}$) was found to be exponentially dependent on RH. $\gamma_{SO2}$ increases from $10^{-3}$ at RH 25% to $10^{-2}$ at RH 71% as measured for a multifunctional organic peroxide. Under similar conditions, the kinetics were found to be structurally dependent: multifunctional organic peroxides have a higher $\gamma_{SO2}$ than those with only one peroxide group, consistent with the reactivity trend observed previously in the aqueous phase. In addition, $\gamma_{SO2}$ is linearly related to particle-phase peroxide content, which in turn depends on gas-particle partitioning of organic peroxides. Aerosol acidity plays a complex role in determining $SO_2$ uptake rate, influenced by the effective Henry's Law constant of $SO_2$ and the condensed phase kinetics of the peroxide-$SO_2$ reaction in the highly concentrated aerosol phase. These uptake coefficients are consistently higher than those calculated from the reaction kinetics in the bulk aqueous phase, and we show experimental evidence suggesting that other factors, such as particle-phase ionic strength, can play an essential role in determining the uptake kinetics. $\gamma_{SO2}$ for different types of secondary organic aerosol (SOA) were measured to be on the order of $10^{-4}$. Overall, this study provides quantitative evidence of the multiphase reactions between $SO_2$ and organic peroxides, highlighting the important factors that govern the uptake kinetics.

https://doi.org/10.5194/acp-2020-983
Preprint. Discussion started: 12 October 2020


Atmospheric Chemistry and Physics Discussions

## Introduction

Sulfate and organic compounds are ubiquitous particulate components in both polluted and pristine environments (Chen et al., 2009;Andreae et al., 2018;He et al., 2011;Sun et al., 2013;Huang et al., 2014), with important implications for public health and global climate (Hallquist et al., 2009). Particulate sulfate can form via S(IV) oxidation by OH radicals in the gas phase and via oxidation in cloud water, fog droplets or the aerosol aqueous phase, including by $H_2O_2$, $O_2$ (catalyzed by transition metals), $O_3$, $NO_2$ and small organic peroxides (methyl hydroperoxide and peroxyacetic acid) (Seinfeld and Pandis, 2012). However, atmospheric models tend to underestimate particulate sulfate production on both global (Tie et al., 2001;Yang et al., 2017;Fairlie et al., 2010) and regional scales, especially during heavy haze episodes (Wang et al., 2014;Zheng et al., 2015;Sha et al., 2019;Gao et al., 2016;Li et al., 2017;Huang et al., 2019), suggesting that the overall kinetics may be underestimated and/or important mechanisms may be missing in models.

To reconcile these differences, studies have investigated novel reaction mechanisms of sulfate formation. Stabilized Criegee intermediates (sCIs) were found to oxidize $SO_2$ rapidly and proposed to be an important source of ambient sulfate (Mauldin et al., 2012). When Liu et al. (2019) applied this mechanism and kinetics to a source-oriented WRF-Chem model, the sCIs pathway was found to only account for at most 9% of the total particulate sulfate. Reactive nitrogen species (such as $NO_2$) have also been put forward to account for the missing sulfate at relatively high aerosol pH (close to 7) (Wang et al., 2016;Cheng et al., 2016). However, such high aerosol pH is not substantiated by thermodynamic models, which conclude that pH ranges between 4 and 5 even in polluted regions (Song et al., 2018;Guo et al., 2017). A recent modeling study incorporating this heterogeneous $NO_x$ mechanism still exhibited a discrepancy of 20%

https://doi.org/10.5194/acp-2020-983
Preprint. Discussion started: 12 October 2020


Atmospheric Chemistry and Physics Discussions

between the predicted and observed sulfate, indicating the possibility of unknown mechanisms (Huang et al., 2019). Other factors may play a role in enhancing the particle-phase sulfate formation rates. Chen et al. (2019) investigated the synergistic effects of $NO_2$ and $NH_3$ on sulfate formation, and found that the rate of this reaction can be enhanced by the high ionic strength in the particle phase. This enhancement effect by solute strength on sulfate formation was also investigated for the $H_2O_2$ pathway in aerosol liquid water. Liu et al. (2020) found ionic strength and general acid-catalyzed mechanisms can cause the S(VI) formation rate to be nearly 50 times faster in aerosol phase than in dilute solutions. On the other hand, during the severe haze episodes in China (Li et al., 2020; Guo et al., 2017), transition metal ion (TMI) catalysis of $SO_2$ oxidation by $O_2$ can be significantly suppressed in the aerosol phase due to high ionic strength (Liu et al., 2020;Cheng et al., 2016; Su et al., 2020).

In addition to high solute strength, submicron aerosol is also rich in organic compounds (Jimenez et al., 2009;Hallquist et al., 2009). In recent years, many studies have investigated the potential role of heterogeneous interactions between $SO_2$ and organic aerosol on particulate sulfate formation. Song et al. (2019) found heterogeneous oxidation of hydroxymethanesulfonate (HMS) by OH can trigger rapid sulfate formation. Wang et al. (2020) studied photosensitizers in ambient particles and found this pathway could be essential under specific light conditions. Recent studies found reactive intermediates from isoprene oxidation (Huang et al., 2019) and benzoic acid (Huang et al., 2020), can yield a variety of organosulfur species upon catalysis by TMI. Other studies have also investigated the interactions between secondary organic aerosol (SOA) and $SO_2$. Field observations found that ambient sulfate abundance is highly correlated with SOA formation (Yee et al., 2020;Xu et al., 2015). Liu et al. (2019) found that $SO_2$ enhances SOA formation and average carbon oxidation state during methoxyphenol photooxidation. By

https://doi.org/10.5194/acp-2020-983
Preprint. Discussion started: 12 October 2020


Atmospheric Chemistry and Physics Discussions

performing chamber experiments with limonene SOA formation in the presence of $SO_2$, Ye et al. (2018) also observed significant $SO_2$ decay along with increased SOA yields and carbon oxidation state, proposing that organic peroxides in SOA may be the key reactive intermediates for $SO_2$ oxidation.

Organic peroxides are key intermediates for aerosol formation and ubiquitously exist in many SOA systems (Hallquist et al., 2009;Bianchi et al., 2019). Numerous studies have reported peroxide content of 20-60% for isoprene and monoterpene derived SOA (Surratt et al., 2006;Ng et al., 2008;Ye et al., 2018;Epstein et al., 2014). A significant fraction of organic peroxide (30%-50%) has also been found in naphthalene-derived SOA under low/high $NO_x$ conditions (Kautzman et al., 2009). Using model simulations, Bonn et al. (2004) found organic hydroperoxides can account for up to 60% of global SOA. The aqueous phase reaction kinetics between organic peroxides and dissolved $SO_2$ have been explored in previous studies (Lind et al., 1987;Gunz and Hoffmann, 1990;Wang et al., 2019;Dovrou et al., 2019;Yao et al., 2019). The second order reaction rate constants for organic peroxides in SOA (Dovrou et al., 2019;Yao et al., 2019) and S(IV) were measured to be on the order of $10^2$-$10^3$ $M^{-1}$ $s^{-1}$, which are within the range of those measured for commercially available organic peroxides (Wang et al., 2019) and small organic peroxides (Lind et al., 1987). Yao et al. (2019) quantified the reactive uptake coefficient of $SO_2$ ($\gamma_{SO2}$) onto α-pinene SOA to be on the order of $10^{-4}$-$10^{-3}$, which is positively dependent on RH and inferred particle-phase peroxide content. These reactions are also linked to the formation of organosulfates (Wang et al., 2019). Both inorganic sulfate (85-90%) and organosulfates (10-15%) were observed as products of $SO_2$ reactive uptake onto SOA (Yao et al., 2019).

https://doi.org/10.5194/acp-2020-983
Preprint. Discussion started: 12 October 2020


Atmospheric Chemistry and Physics Discussions

92 Given the potential significance of $SO_2$ reactive uptake in particulate sulfate formation, a more
93 in-depth study is needed to determine the important factors that govern the heterogeneous
94 kinetics of $SO_2$ onto organic peroxide containing aerosol. In this study, we measured $\gamma_{SO2}$ for two
95 categories of aerosol: 1. Model organic peroxides mixed with ammonium sulfate or malonic acid
96 and 2. SOA from a few representative biogenic and anthropogenic precursors. The impacts of
97 RH, peroxide type, peroxide content, and condensed phase pH on $SO_2$ reactive uptake were
98 evaluated systematically with the goal of better understanding atmospheric multiphase sulfate
99 formation.
100
101 **2. Methods**
102 The reactive uptake of $SO_2$ onto peroxide-containing particles was studied in a 1 $m^3$ Teflon
103 chamber under ambient temperature and pressure. In brief, generated particles and $SO_2$ were
104 introduced into the chamber separately. The consumption of $SO_2$, changes in particle size
105 distribution and chemical composition were monitored to estimate the reactive uptake
106 coefficients. Particles were also collected on filters for offline chemical characterization.
107
108 **2.1 Seed aerosol generation**
109 In this work, two types of aerosol were used to investigate the uptake of $SO_2$. The first is
110 ammonium sulfate or malonic acid mixed with model organic peroxides (Fig. S1). In this first set
111 of experiments, an aerosol atomizer (Model 3076, TSI Inc., USA) was used to generate aqueous
112 particles from dilute solution. Each solution consists of ammonium sulfate (≥99%, Sigma-
113 Aldrich) or malonic acid (99%, Sigma-Aldrich) and a model organic peroxide in ultrapure water
114 (HPLC grade, Fisher Chemical). For the experiments investigating the relationship between $\gamma_{SO2}$

https://doi.org/10.5194/acp-2020-983
Preprint. Discussion started: 12 October 2020


Atmospheric Chemistry and Physics Discussions

and peroxide type (Expt. 2-14), different commercially available organic peroxides were used, including tert-butyl hydroperoxide (70 wt. % in water, Sigma-Aldrich), cumene hydroperoxide (80 wt. % in water, Sigma-Aldrich), and 2-butanone peroxide (40% wt. % in water, Sigma-Aldrich). The molar ratio of organic peroxide to ammonium sulfate in the atomizing solution was 2:1 with the aim of being atmospherically relevant (corresponding to maximum particulate peroxide molar fraction of 66% and mass fraction of approximately 50-70% if all the organic peroxides were assumed to remain in the particle phase). This ratio was used as a proxy for total peroxide content in both gas and particle phase relative to that of ammonium sulfate upon atomization. For the experiments studying the relationship between $\gamma_{SO2}$ and particle-phase peroxide content, the molar ratio of organic peroxide to ammonium sulfate (Expt. 10-12, 15-18) in the solution was adjusted to be 0.02, 0.2, 1, 2, and 4, respectively. In experiments where malonic acid was used (Expt. 19-22), molar ratios of 0.2, 1, 2, and 4 were adopted. For measuring $\gamma_{SO2}$ with different aerosol pH (Expt. 17, 23-25), different amounts of HCl (37%, Sigma-Aldrich) were added into the solution prior to atomization. The atomized particles were flowed into the chamber without drying, and therefore assumed to remain deliquesced under the range of RH we studied. Expt. 2-14 also represent those where the relationship between $\gamma_{SO2}$ and RH conditions were studied.

In the second set of experiments, the uptake of $SO_2$ onto SOA was investigated (Fig. S2, Expt. 26-28). A custom-built 10 L quartz oxidation flow reactor was used to produce SOA (Ye et al., 2016) from different hydrocarbon precursors. In this work, we studied SOA formed from toluene photooxidation, limonene ozonolysis and α-pinene ozonolysis, 3 of the most commonly studied SOA systems (Ng et al., 2007;Hildebrandt et al., 2009; Hartz et al., 2005;Varutbangkul et al., 2006). Toluene (analytical standard, Sigma Aldrich) was injected continuously into zero air flow

https://doi.org/10.5194/acp-2020-983
Preprint. Discussion started: 12 October 2020


Atmospheric Chemistry and Physics Discussions

by a syringe (1000 mL, Hamilton) installed on a syringe pump (KDS Legato100) to achieve an initial concentration of 0.5 ppm. Limonene (Sigma-Aldrich, 97 %) and α-pinene (Sigma-Aldrich, 98 %) were pre-dissolved in cyclohexane (Sigma-Aldrich, 99.5 %) with a volumetric ratio of 1: 1500 and 1: 500 to ensure that OH formed from limonene or α-pinene ozonolysis is scavenged by cyclohexane, estimated based on the rate constants (Atkinson and Arey, 2003). The initial steady-state concentrations of limonene and α-pinene were controlled to be around 2 ppm and 1 ppm entering the flow tube. $O_3$, used as the oxidant (for limonene and α-pinene) or the OH precursor (for toluene), was generated by passing 0.5 L $min^{-1}$ pure oxygen (99.6 %, Linde, Mississauga, Canada) through an $O_3$ generator (no. 97006601, UVP, Cambridge, UK). Humidified air was produced by bubbling zero air through a custom-made humidifier at a flow rate of 1 L $min^{-1}$. The photolysis of $O_3$ produces O ($^1$D), which reacts with water vapour to produce ·OH with illumination from the 254 nm UV lamps (UVP, Cambridge, UK) to initiate the photooxidation of toluene. The average residence time inside the flow tube was controlled to be around 5 minutes. A gas chromatography–flame ionization detector (GC-FID, model 8610C, SRI Instruments Inc., LV, USA) equipped with a Tenax® TA trap was used to monitor the concentration of hydrocarbon precursors at the inlet/outlet of the flow reactor. In all cases, the $O_3$ concentration was maintained to be at least 10 times higher than that of the hydrocarbon. Temperature and relative humidity were monitored by an Omega HX94C RH/T transmitter. Particle size distribution and volume concentration were monitored using a custom-built scanning mobility particle sizer (SMPS), which is a combination of a differential mobility analyzer column (DMA, model 3081, TSI, Shoreview, MN, USA) with flow controls and a condensation particle counter (CPC, model 3772, TSI, Shoreview, MN, USA).

https://doi.org/10.5194/acp-2020-983
Preprint. Discussion started: 12 October 2020


Atmospheric Chemistry and Physics Discussions

161 **2.2 Quantification of $\gamma_{SO2}$**

162 Prior to each experiment, the chamber was flushed by purified air overnight with a flow rate of
163 25 L $min^{-1}$ until particle number concentration was less than 5 $cm^{-3}$ and $SO_2$ was less than 1 ppb.
164 To adjust RH, the chamber was humidified by passing purified air through a custom-built
165 humidifier filled with ultra-pure water. For experiments with atomized ammonium sulfate or
166 malonic acid, $SO_2$ was injected into the chamber prior to the introduction of particles. For
167 experiments studying $\gamma_{SO2}$ onto SOA, aerosol generated from the flow tube was injected into the
168 Teflon chamber continuously after passing through an $O_3$ denuder (Ozone Solutions, Iowa, USA)
169 to achieve specific aerosol concentration inside the chamber prior to $SO_2$ addition. $SO_2$ mixing
170 ratio in the chamber during each experiment was continuously monitored using an $SO_2$ analyzer
171 (Model 43i, Thermo Scientific). The initial mixing ratio of $SO_2$ in each experiment was
172 controlled to be around 200 ppb. Aerosol size distribution was monitored by SMPS. The reactive
173 uptake coefficient of $SO_2$ was calculated by integrating the following equation:

174 $$-\frac{d[SO_2]}{dt} = \frac{1}{4}\gamma_{SO_2} A\bar{c}[SO_2] \quad (1)$$

175

176 Where $[SO_2]$ is the $SO_2$ mixing ratio (ppb) monitored by the $SO_2$ analyzer; A is the average
177 surface area concentration ($\mu m^2$ $cm^{-3}$) derived from the particle size distribution measured by
178 SMPS; $\bar{c}$ represents the mean molecular velocity (cm $s^{-1}$) of $SO_2$. $d[SO_2]/dt$ is solved over the
179 initial $SO_2$ decay, such that the peroxide concentration in the aerosol liquid phase is assumed to
180 be constant and pseudo-first order kinetics can be applied (Abbatt et al., 2012;Thornton et al.,
181 2003). A summary of all the measured $\gamma_{SO2}$ can be found in Table S1. Typical evolution of
182 monitored species can be seen in Fig.1. Control experiments were performed in order to rule out
183 other potential factors (e.g. $SO_2$ loss in the in-line filter in front of the $SO_2$ analyzer, interferences
184 inside the $SO_2$ analyzer, chamber wall losses, $SO_2$ uptake onto wet ammonium sulfate, gas-phase

https://doi.org/10.5194/acp-2020-983
Preprint. Discussion started: 12 October 2020


Atmospheric Chemistry and Physics Discussions

185 reaction of $SO_2$ with peroxide vapour) that may contribute to the $SO_2$ decay observed during the
186 $\gamma_{SO2}$ measurement inside the chamber (Fig. S3-S6). Measurement uncertainty of $\gamma_{SO2}$ in this study
187 was estimated from Expt. 10-12 to be 26%. Also, we observed there was $SO_2$ repartitioning from
188 the humid chamber wall in the presence of organic peroxide under high RH (Fig. S6b, RH 74%).
189 The observed $SO_2$ repartitioning rate was then applied to correct the $\gamma_{SO2}$ measured under high
190 RH conditions (above 70%, Expt.14), and this correction amounts to a 40% increase in
191 calculated $\gamma_{SO2}$.
192
193 **2.3 Offline peroxide quantification**
194 Aerosol was collected onto 47 mm PTFE (polytetrafluoroethylene) filters with 0.2 μm pore size
195 (Whatman®, GE Healthcare) from the chamber by a diaphragm pump (KNF Neuberger Inc.,
196 USA) for offline chemical analysis. The particulate peroxide content in these samples prior to
197 $SO_2$ uptake was quantified using the iodometric–spectrophotometric assay (Docherty et al.,
198 2005). $I_2$ produced from the reaction between $I^-$ and peroxides can further quickly combine with
199 the excess amount of $I^-$ to form $I_3^-$, which has brown color and absorbs UV-vis at 470nm. The
200 SOA extraction was then aliquoted into a 96-well UV plate (Greiner Bio-One, Kremsmünster,
201 AT) with 160 μL $well^{-1}$. 20 μL of formic acid (⩾ 95 %, Sigma-Aldrich) was added into each
202 well, following by 20 μL potassium iodide (BioUltra, ⩾99.5%, Sigma-Aldrich) solution
203 (dissolved in DI water). The plate was then covered by an adhesive plate sealer (EdgeBio,
204 Gaithersburg, USA) immediately in order to avoid reagent evaporation and $O_2$ oxidation. After
205 incubation for an hour in the dark, the UV-vis absorption at 470nm was measured using a UV-
206 vis spectrophotometer (Spectramax 190, Molecular Devices Corporation, Sunnyvale, CA) and
207 then converted to peroxide concentration using the calibration curve made by tert-butyl

https://doi.org/10.5194/acp-2020-983
Preprint. Discussion started: 12 October 2020


Atmospheric Chemistry and Physics Discussions

hydroperoxide (70 wt. % in $H_2O$, Sigma-Aldrich) with a series of concentrations (0-10mM). The average molecular mass for aerosol was assumed based on the chemical composition in order to calculate the molar fraction of total peroxides. More details about the iodometric-spectrophotometric procedures were described in previous work (Wang et al., 2018).

## 3 Results and discussion

### 3.1 $SO_2$ uptake and RH

A positive relationship between $\gamma_{SO2}$ and RH (between 25 and 71%) was observed for all types of organic peroxides studied (Fig. 2). The positive dependence of the reactive uptake coefficient of water-soluble gaseous species on RH has also been observed in other studies (Thornton et al., 2003;Griffiths et al., 2009;Zhao et al., 2017;Zhang et al., 2019). Recently, the uptake behavior of $SO_2$ onto soot, mineral dust and SOA were also shown to positively depend on RH (Zhang et al., 2019;Zhao et al., 2017;Yao et al., 2019).

It is also noteworthy that an exponential dependence of $SO_2$ reactive uptake coefficient on RH was observed in our study. $\gamma_{SO2}$ increases with increased relative humidity, which could even be more significant under high RH regime. This is consistent with previous laboratory studies that measured the reactive uptake coefficient of $SO_2$ onto aerosol to be exponentially dependent on RH (Zhang et al., 2019;Yao et al., 2019). Additionally, multiple field campaigns have observed significant correlation between particulate sulfate formation and ambient RH (Song et al., 2019;Sun et al., 2013;Huang et al., 2020). Sun et al. (2013) observed faster sulfate formation rate under humid conditions, proposing a significant impact of aerosol liquid water on sulfate production during wintertime in Beijing. Zheng et al. (2015) reported a notably higher SOR (molar ratio of sulfate to the sum of sulfate and $SO_2$) during wet period (RH>50%), indicating

https://doi.org/10.5194/acp-2020-983
Preprint. Discussion started: 12 October 2020


Atmospheric Chemistry and Physics Discussions

the importance of heterogeneous reactions to the secondary sulfur transformation with abundant aerosol water content under humid conditions. In a recent study by Song et al. (2019), the rapid sulfate formation rate observed under high RH conditions was found to be significantly higher than atmospheric modeling results implemented with homogeneous $SO_2$ oxidation pathways, which was later attributed to heterogeneous sulfate formation mechanisms. Multiple mechanisms can potentially explain this observed $\gamma_{SO2}$-RH dependence. An enhanced relative humidity would result in a nonlinear increase of aerosol water content, which can lead to more $SO_2$ dissolved in the aerosol aqueous phase (Seinfeld and Pandis, 2012). It should be noted that while the relative humidity is varied systematically in these experiments, the relationship is more complex since RH also affects other aerosol properties which can affect the uptake kinetics in turn. For example, a higher aerosol liquid water content could dilute protons and thus lower the aerosol acidity. In a study by Laskin et al. (2003), an enhanced uptake of $SO_2$ onto sea-salt particles was observed with an increased aerosol alkalinity at high pH range.

### 3.2 Dependence of $SO_2$ uptake on peroxide content and type

As expected, the measured uptake rate of $SO_2$ is dependent on the particulate peroxide content in the current study. Fig. 3 shows that $\gamma_{SO2}$ is linearly proportional to the amount of particulate peroxide for aerosol with similar volume-to-surface ratios and containing the same type of organic peroxides. This positive relationship between $\gamma_{SO2}$ and condensed phase peroxide content has also been inferred from experiments of $SO_2$ uptake onto α-pinene SOA (Yao et al., 2019), where the peroxide content in α-pinene SOA was varied indirectly by introducing NO and adjusting the branching ratio of the peroxide-yielding $RO_2$+$HO_2$/$RO_2$ pathway.

https://doi.org/10.5194/acp-2020-983
Preprint. Discussion started: 12 October 2020


Atmospheric Chemistry and Physics Discussions

In addition to the amount of peroxide injected, the particulate fraction of organic peroxide available for heterogeneous reaction is also influenced by gas-particle partitioning. As indicated in Fig. 2, the reactive uptake coefficients of different organic peroxides vary amongst each other by about an order of magnitude in the range of RH studied, despite the same amounts of peroxide relative to ammonium sulfate initially in the atomizing solution. Based on our previous work (Wang et al., 2019), the aqueous-phase rate constants for these organic peroxides with dissolved S(IV) only vary by a factor of 2-3 and therefore cannot fully explain the observed difference in uptake rates. Since vapour pressure vary considerably among the different peroxides in the present study, gas-particle partitioning is likely to influence the amount of peroxide in the particle phase that react with dissolved $SO_2$. The relative particulate peroxide content on filters of the three peroxides collected from chamber experiments under RH 50% without $SO_2$ uptake were measured by the offline KI method (Fig. S7). Although the initial ratio of organic peroxide to ammonium sulfate in the atomizing solution was nominally the same, we measured the highest amount of particulate peroxide with 2-butanone peroxide (16.7%), followed by cumene hydroperoxide (12.7%) and then tert-butyl hydroperoxide (3.8%) using the offline iodometric method. This trend in particulate peroxide content is consistent with the vapour pressures calculated using the SIMPOL group contribution method (Pankow et al., 2008), with 2-butanone peroxide being the least volatile, and tert-butyl hydroperoxide being the most volatile. Also, the order of particle-phase peroxide content is consistent with the order of $\gamma_{SO2}$ observed, as shown in Fig. 2. A simple visualization of these relationships between different peroxide characteristics (number of peroxide groups, vapour pressure and aqueous-phase rate constants) and measured $\gamma_{SO2}$ (at RH = 50%) is illustrated in Fig. S7, which indicates higher $\gamma_{SO2}$ can be expected for multifunctional organic peroxides with lower vapour pressures and higher aqueous phase

https://doi.org/10.5194/acp-2020-983
Preprint. Discussion started: 12 October 2020


Atmospheric Chemistry and Physics Discussions

reactivities. It should be noted that the order of magnitude difference in experimentally measured $\gamma_{SO2}$ among various organic peroxides (Fig.2) is still not fully explained when both volatility and reaction kinetics are taken into account (Fig.S7), suggesting that the reactive uptake may be influenced by other factors. In summary, for our current experiments where we nominally maintained total injected amount of organic peroxide constant, measured $\gamma_{SO2}$ depends both on reactivity and gas-particle partitioning of the organic peroxides.

### 3.3 $SO_2$ uptake and aqueous phase kinetics

Since the aqueous phase reaction rate constants between S(IV) and these model organic peroxides have been measured previously (Wang et al., 2019), we can test our understanding of the measured $\gamma_{SO2}$ using a simple model. By assuming the amount of $SO_2$ dissolved in the aerosol is in equilibrium with the gas phase, the overall $\gamma_{SO2}$ can be expressed using the simplified resistor model (Hanson et al., 1994):

$$\frac{1}{\gamma} = \frac{1}{\alpha} + \frac{\bar{c}}{4HRT\sqrt{k^l D_l}} \frac{1}{\left[\coth(q) - \frac{1}{q}\right]} \quad (2)$$

where α is the mass accommodation coefficient, $\bar{c}$ is the mean molecular speed of $SO_2$ (cm $s^{-1}$), H is the effective Henry's law constant that includes both the dissolution of $SO_2$ and the dissociation of $H_2SO_3$ (M $atm^{-1}$), R is the ideal gas constant (atm L $mol^{-1}$ $K^{-1}$), T is the temperature (K), and the parameter q is used to describe the competition between the reaction and diffusion of the dissolved gaseous species within a particle, which is further calculated as:

$$q = r\sqrt{\frac{k^I}{D_l}} \quad (3)$$

where r is the radius (cm) of a given particle, $D_l$ is the aqueous-phase diffusion coefficient ($cm^2$ $s^{-1}$), $k^I$ is the first order rate constant ($s^{-1}$) for the reaction. For experiments in the current study,

https://doi.org/10.5194/acp-2020-983
Preprint. Discussion started: 12 October 2020


Atmospheric Chemistry and Physics Discussions

299 the calculated q values were consistently found to be far less than 1, which indicates a volume-
300 limited reaction regime. Combining with the assumption of a relatively fast mass
301 accommodation process compared with the bulk phase reaction, equation (2) can be further
302 simplified as to describes reactive uptake in the volume-limited regime:

303 $$\gamma = \frac{4HRT[peroxide]k^{II}}{\bar{c}}\frac{V}{S} \quad (4)$$

304 Here, we assume all the peroxides remain in the condensed phase upon atomizing and reaction
305 inside the chamber for the upper-bound prediction of $\gamma_{SO2}$. [peroxide] represents the particle phase
306 concentration of total organic peroxide (M) based on the initial ratio between organic peroxide and
307 ammonium sulfate in the atomizing solution, and the aerosol water content output by E-AIM III
308 (Clegg et al., 1998), $k^{II}$ is the second order reaction rate constant ($M^{-1}$ $s^{-1}$), which we have
309 measured in the bulk phase at dilute concentrations previously (Wang et al., 2019), V/S is the ratio
310 between particle volume concentration ($\mu m^3$ $cm^{-3}$) and particle surface area concentration ($\mu m^2$
311 $cm^{-3}$) derived from SMPS measurements. As a result, the observed reactive uptake coefficient of
312 $SO_2$ can be compared to that predicted from the bulk phase reaction rate constant, and the results
313 are shown in Fig. 4 and Fig. S8. Overall, we noticed that this model captures the dependence of
314 $\gamma_{SO2}$ on peroxide content, but the modeled results were found to be generally 15-50 times lower
315 than the experimentally measured values (Fig. S8). The current $\gamma_{SO2}$ predictions are likely upper-
316 bound estimates since all the peroxides were assumed to stay in the condensed phase without
317 partitioning. As a result, this observed 15-50 times of discrepancy could even be larger if the
318 particulate peroxide content during the chamber experiments were lower due to partitioning.
319 It should be noted that the calculated $\gamma_{SO2}$ was based on reaction kinetics measured in dilute
320 solutions while the experimental $\gamma_{SO2}$ were measured directly from suspended particles. This large
321 difference in kinetics between those in aerosol and in dilute bulk solution suggests that this

https://doi.org/10.5194/acp-2020-983
Preprint. Discussion started: 12 October 2020


Atmospheric Chemistry and Physics Discussions

multiphase interaction is strongly favored in the highly concentrated aerosol environment. One of the potential explanations for this discrepancy could be liquid-liquid phase separation (LLPS) in aerosol between organic peroxide and ammonium sulfate (Ciobanu et al., 2009;O'Brien et al., 2015) such that $SO_2$ can directly interact with the acidic organic phase, where the concentration of peroxides can be higher and the kinetics can be different from what we have measured in dilute solution (Wang et al., 2019). However, LLPS is generally governed by the chemical composition of the hydrophobic phase (Freedman, 2017). A higher level of oxygenation in organic aerosol is related with higher hydrophilicity, which would favor a homogeneous particle instead of phase separation. Previous studies showed that LLPS did not occur for organic coating with O:C above 0.8 (You et al., 2013;You et al., 2014). The LLPS phenomenon in simple organic–inorganic mixtures can also be affected by the functional groups. The maximum O:C for LLPS could be 0.71 for organics with multiple carboxylic and hydroxyl groups but low aromatic content (Song et al., 2012) while the 2-butanone peroxide we used for both $\gamma_{SO2}$ measurement and prediction in the present study has multiple peroxide groups with an O:C value of 0.75. Particle size could also have impacts on phase separation (Cheng et al., 2015). Particle diameters in the current study are mainly under 200 nm while a previous study showed particles smaller than this size are less likely to experience LLPS (Veghte et al., 2013). We therefore believe that LLPS is not likely to be responsible for the enhanced uptake rate observed under these experimental conditions.

Another explanation is the high solute strength in the concentrated aerosol phase. As indicated in Fig. 4 and Fig. S8, the difference between the measured and predicted $\gamma_{SO2}$ is larger for ammonium sulfate aerosol than for malonic acid. Meanwhile, the calculated ionic strength in aerosol liquid phase under RH 50% for ammonium sulfate (40 mol $kg^{-1}$) is significantly larger than that of malonic acid (0.45 mol $kg^{-1}$). It has been previously reported that the reaction rate between sulfite

https://doi.org/10.5194/acp-2020-983
Preprint. Discussion started: 12 October 2020


Atmospheric Chemistry and Physics Discussions

and hydrogen peroxide in aqueous phase increases with ionic strength (Maaß et al., 1999). Based on the reaction mechanisms proposed for dissolved $SO_2$ and hydrogen peroxide (Halperin and Taube, 1952), we speculate the reaction between aqueous phase S(IV) and organic peroxides to follow a similar mechanism:

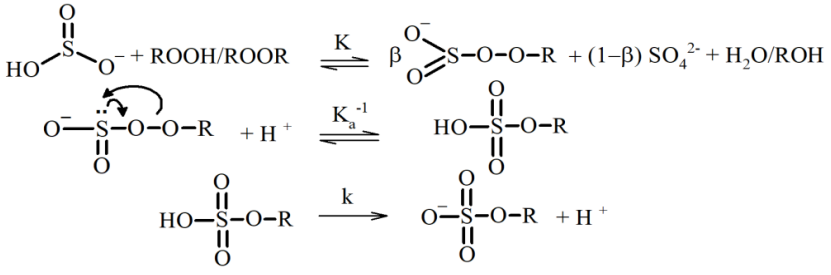


where the overall rate constant is equal to $k\frac{K}{K_a}$, assuming fast equilibrium steps for reactions 5 and 6. Dissociated solutes are surrounded by an extended solvation shell which could affect the reaction rates (Herrmann, 2003). Fewer available free water molecules would therefore shift the equilibrium to the right in equation (5). Additionally, higher ionic strength also corresponds to an increased concentration of electrolytes in the aqueous phase, which could hinder the dissociation of the peroxymonosulfurous acid and shift the equilibrium in equation (6) to the right. In recent work by Liu et al. (2020), the rate of S(IV) oxidation by $H_2O_2$ can be enhanced by up to a factor of 50 in aerosol aqueous phase compared to that of dilute solution. The highest ionic strength at which such enhancement was measured for the $H_2O_2$ oxidation pathway was 15 mol $kg^{-1}$ (Liu et al., 2020).

Whereas the above analysis is based on the assumption that all the chemistry occurs in the bulk component of the particle, it is also possible that some component of the reaction occurs at the gas-particle interface and the overall kinetics can be affected by interfacial characteristics. For example, an enhanced ionic strength in the aerosol phase can also impact the interfacial reaction mechanisms. Previous study has shown evidence that interfacial chemistry is important for $SO_2$ oxidation in the

https://doi.org/10.5194/acp-2020-983
Preprint. Discussion started: 12 October 2020


Atmospheric Chemistry and Physics Discussions

aerosol phase (Laskin et al., 2003). With higher ionic strength, anions partitioning to the air-liquid interface can promote the overall reaction kinetics via proton transfer and thus accelerate the interfacial chemistry (Knipping et al., 2000;Mishra et al., 2012;Mekic et al., 2018;Mekic et al., 2020; Wei et al., 2018; Ruiz-Lopez et al., 2020). However, it should be noted that there is no evidence from the current study showing direct relationship between the interfacial properties and $\gamma_{SO2}$, and future studies are warranted.

Therefore, while more studies are needed to clearly delineate the roles of ionic strength, interfacial activity, bulk reactivity, and particle phase state quantitatively, the enhancement of $SO_2$ oxidation kinetics by highly concentrated aerosol particles compared to dilute aqueous solutions are concluded to be large (factor of 15-50) for the experimental conditions in the current study.

### 3.4 $SO_2$ uptake and aerosol pH

As indicated by the proposed reaction mechanisms (Eqn. 5-7), protons are important reaction intermediates for this $SO_2$ oxidation pathway. Previously, the aqueous phase reaction rate constants between organic peroxides and dissolved $SO_2$ were measured to be pH dependent (Wang et al., 2019). Moreover, the dissolution equilibrium of $SO_2$ into aqueous phase is also pH sensitive (Seinfeld and Pandis, 2012). Besides, many studies have shown that the uptake kinetics for gaseous species can be affected by the condensed phase pH (Shi et al., 1999;Gaston et al., 2014;Drozd et al., 2013;Jang and Kamens, 2001;Liu et al., 2015). Reactive uptake of ammonia was observed to depend on condensed phase acidity (Shi et al., 1999). Heterogeneous condensation of isoprene-derived epoxydiol onto seed aerosol was found to increase with proton concentration (Gaston et al., 2014). In the current study, the potential impact from particle phase pH on $\gamma_{SO2}$ was explored by adding HCl into the atomizing solution. To estimate the particle

https://doi.org/10.5194/acp-2020-983
Preprint. Discussion started: 12 October 2020


Atmospheric Chemistry and Physics Discussions

phase pH, two different methods associated with two different assumptions were used. In the first scenario, the aerosol pH in each experiment was estimated using the E-AIM III model (Clegg et al., 1998) based on the initial molar ratios of inorganic species ($H^+$, $NH_4^+$, $SO_4^{2-}$, $Cl^-$) in the atomizing solution and measured RH (around 50%). In the second scenario, the additional sulfate formed from reactive uptake of $SO_2$ was taken into consideration. The partitioning of HCl was allowed in the model simulation for both scenarios. The formation of sulfate would enhance the proton concentration in the aerosol liquid phase thus lower the aerosol pH. The average pH during the $SO_2$ uptake process is likely in between these two extremes.

Fig. 5 shows the measured reactive uptake coefficients of $SO_2$ as a function of the calculated pH. The reactive uptake coefficient was found to increase with increasing proton concentrations (decreasing pH), which is consistent with acid-catalyzed reactions between peroxides and dissolved $SO_2$ as measured in the bulk phase (Lind et al., 1987; Wang et al., 2019). $\gamma_{SO2}$ was also predicted for the same range of pH based on Eqn. 4 and the pH-dependent bulk-phase reaction rate constants measured previously (Wang et al., 2019). Indicated by Fig. 5, the measured $\gamma_{SO2}$ again exceeds the predicted $\gamma_{SO2}$ by about a factor of 50, which is consistent with what we reported earlier and is likely due to the effects of aerosol ionic strength.

Unlike the observed $\gamma_{SO2}$, however, the predicted $\gamma_{SO2}$ does not exhibit a monotonic trend. $\gamma_{SO2}$ is expected to decrease with decreasing pH at high pH (>2) as the effective Henry's law constant of $SO_2$ decreases with higher acidity (Seinfeld and Pandis, 2012). $\gamma_{SO2}$ is not expected to increase with decreasing pH until pH is below 2 where the acidity enhancement in reaction rate constant exceeds the decrease in $SO_2$ solubility. As illustrated earlier, extrapolating dilute aqueous-phase kinetics to the highly concentrated aerosol requires considering effects from high solute strength. Solute strength may change the pH dependence of $\gamma_{SO2}$ in two ways. First, the solubility of $SO_2$

https://doi.org/10.5194/acp-2020-983
Preprint. Discussion started: 12 October 2020


Atmospheric Chemistry and Physics Discussions

410 may decrease and become less dependent on pH as ionic strength increases (Rodríguez-Sevilla et
411 al., 2002). A former study (Leng et al., 2015) has shown that the effective Henry's law of
412 triethylamine decreases with increased ionic strength. Another potential explanation is that the
413 aqueous phase reaction rate constant can be more pH-dependent at high ionic strengths than what
414 we measured previously in dilute solutions. In either case, the inflection of the predicted $\gamma_{SO2}$
415 would change and $\gamma_{SO2}$ could become more negatively dependent on pH (d[$\gamma_{SO2}$]/d[pH] becomes
416 less positive in the high pH range and/or more negative in the low pH range), which would
417 match more closely with the observed dependence. It should also be noted that there are
418 substantial uncertainties in estimating pH values since the reactive uptake is a dynamic process
419 and will influence aerosol pH in turn upon sulfate formation. In summary, while the magnitude
420 of predicted $\gamma_{SO2}$ is consistent with our expected values (after accounting for the enhancement by
421 high aerosol solute strength), we cannot fully explain the dependence of $\gamma_{SO2}$ on aerosol pH at the
422 current stage. Future studies should investigate how the effective Henry's law of $SO_2$ and pH
423 dependence of reaction rate constants vary in aerosol liquid phase with high solute strength in
424 order to have a more comprehensive understanding of the relationship between $\gamma_{SO2}$ and aerosol
425 pH.

426 **3.4 $SO_2$ uptake onto SOA**

427 $\gamma_{SO2}$ was measured for a few model SOA systems, as organic peroxides are abundant in SOA
428 (Surratt et al., 2006;Kautzman et al., 2009;Krapf et al., 2016;Bonn et al., 2004). Here we studied
429 SOA formed from monoterpene ozonolysis and toluene photooxidation. It should be noted that
430 for the $\gamma_{SO2}$ measurements of toluene SOA, a strong hydrocarbon interference was observed with
431 the $SO_2$ analyzer, likely stemming from the high concentrations of gas-phase aromatic
432 compounds. A rough estimate of the uptake rate for toluene SOA from aerosol mass

https://doi.org/10.5194/acp-2020-983
Preprint. Discussion started: 12 October 2020


Atmospheric Chemistry and Physics Discussions

spectrometer sulfate measurements is provided in the SI (Section 1). The reactive uptake coefficient of $SO_2$ onto Saharan mineral dust was reported on the order of $10^{-5}$ (Adams et al., 2005). $\gamma_{SO2}$ onto dust with the coexistence of $NO_2$ and $NH_3$ under various RH conditions were measured to be $10^{-7}$ to $10^{-5}$ (Zhang et al., 2019). For a variety of metal oxides, $SO_2$ reactive uptake coefficients were quantified to be between $10^{-6}$ and $10^{-4}$ (Usher et al., 2002; Fu et al., 2007; Shang et al., 2010). More recently, $\gamma_{SO2}$ studied for heterogeneous sulfate formation by photolysis of particulate nitrate were reported in the range of $10^{-6}$ to $10^{-5}$ (Gen et al., 2019). As shown in Fig. 6, $\gamma_{SO2}$ for all SOA systems were measured to be on the order of $10^{-4}$. Similar $\gamma_{SO2}$ values on the order of $10^{-4}$ were measured for α-pinene SOA by Yao et al. (2019), and $10^{-5}$ for limonene SOA estimated from the chamber study by Ye et al. (2018). The reaction products from this SOA and $SO_2$ interaction will be reported in a separate study.

## 4. Atmospheric Implications

Oxidation of atmospheric hydrocarbons produces reactive intermediates that can potentially interact with $SO_2$ and form particulate sulfate, contributing to PM formation and growth (Berndt et al., 2015;Mauldin et al., 2012;Yao et al., 2019). Organic peroxides generated from both biogenic and anthropogenic hydrocarbon emissions are abundant in submicron aerosol. Given that they are highly reactive with relatively short lifetimes (Bonn et al., 2004;Krapf et al., 2016;Qiu et al., 2020), these species could serve as important condensed phase oxidants for gas phase $SO_2$. Combining laboratory measurements and model predictions, the current study investigated heterogeneous reactions between $SO_2$ and particulate organic peroxide. The measured $\gamma_{SO2}$ for organic peroxide containing aerosol ranges from $10^{-5}$ to $10^{-2}$ in this study. Based on the modeling work by Wang et al. (2014), adding an $SO_2$ uptake pathway to GEOS-

https://doi.org/10.5194/acp-2020-983
Preprint. Discussion started: 12 October 2020


Atmospheric Chemistry and Physics Discussions

Chem with a reactive uptake coefficient of $10^{-4}$ could improve the surface sulfate prediction by more than 50% during a severe haze episode over North China (RH 50%), suggesting the potential importance of this multiphase reaction pathway, especially when SOA is the dominant component in particulate matter.

The dependence of the heterogeneous kinetics on RH, aerosol pH, peroxide type, and peroxide content were also evaluated. The experimentally measured $\gamma_{SO2}$ was found to be consistently higher than that predicted from reaction kinetics with organic peroxides in the dilute aqueous phase. This discrepancy can be potentially explained by the effects of high ionic strength presented in the aerosol, suggesting that the impact from highly concentrated solutes needs to be taken into consideration when applying aqueous phase kinetics to aerosol multiphase chemistry, especially for particles containing strong electrolytes. We also observed that the kinetics of this multiphase reaction exhibit a weak dependence on pH. Increasing the condensed-phase acidity enhances the heterogeneous rate constant at low pH range, and while this pH dependence is consistent with that of the aqueous phase reaction rate constant measured previously, it is not consistent with the decrease of effective Henry's law constant of $SO_2$ along with enhanced acidity. Currently, we are not able to fully explain the pH dependence, likely due to the uncertainties from high ionic strength, and further studies are warranted. Particle phase peroxide content was observed to be linearly correlated with $\gamma_{SO2}$. Moreover, $\gamma_{SO2}$ measured for 2-butanone peroxide was found to be orders of magnitude higher than that of cumene hydroperoxide and tert-butyl hydroperoxide. The difference in $\gamma_{SO2}$ among various types of organic peroxides can be partially explained by their condensed-phase reactivity and gas-particle partitioning.

In general, we found the observed $\gamma_{SO2}$ in this study can be summarized using the following semiempirical multilinear relationship:

https://doi.org/10.5194/acp-2020-983
Preprint. Discussion started: 12 October 2020


Atmospheric Chemistry and Physics Discussions

$$\log \gamma = -1.7 + 0.0024 \times k^{II} + 0.46 \times PAS + 0.024 \times RH - 1.9 \times Vp \quad (8)$$

where $\gamma$ is the reactive uptake coefficient, $k^{//}$ is the aqueous phase S(IV) oxidation rate constant ($M^{-1}$ $s^{-1}$) , $PAS$ is the molar ratio between particulate peroxide and ammonium sulfate in the atomizing solution, which is a proxy for the amount of peroxide in both gas and particle phases applied in the current study, $RH$ is the relative humidity (%),$Vp$ is the vapour pressure (kPa) of the peroxide. Fig. 7 illustrates the degree to which this semi-empirical expression describes the experimental data for ammonium sulfate aerosol mixed with the three types of organic peroxides. Residual evaluations of this multilinear regression can be found Fig. S9. We caution that this equation is not directly applicable to atmospheric models in its current form, especially since the particle phase peroxide content (PAS) value we applied as input is a calculated value, rather than a measurement. However, it illustrates the internal consistency of our experimental results across a range of RH, peroxide content, and aqueous phase reactivities, which are the key variables for uptake rates. Better understanding of ionic strengths and pH in aerosol, either through modeling or direct measurements of these variables, is needed to establish the coefficient dependence. Future studies should be focused on exploring $\gamma_{SO2}$ and the reaction products for various types of SOA as well as ambient particles under atmospherically relevant conditions, evaluating the underlying impacts from photochemical condition, chemical composition, particle morphology, ionic strength and interfacial properties on this multiphase physicochemical process. Overall, $\gamma_{SO2}$ presented in our study and its relationship with ambient RH, aerosol pH, ionic strength, particulate peroxide content and type could provide a framework for the implementation of this heterogeneous mechanism in atmospheric models to have a better understanding of ambient sulfate formation and particle growth.

https://doi.org/10.5194/acp-2020-983
Preprint. Discussion started: 12 October 2020


Atmospheric Chemistry and Physics Discussions

*Author contributions*

A.W.H. C. and S.W. designed the study. S.W., T. L., and J. J. performed the experiments. S.W., A.W.H. C., T. L., and J. J. analyzed data. S.W. and A.W.H. C. wrote the manuscript with the input from all co-authors.

*Data availability*

All data presented in this study are available in the supplemental material and have been deposited in figshare.

*Associated content*

Supporting Information.

*Competing interests*

The authors declare no competing financial interest.

*Acknowledgements*

This work was supported by Natural Sciences and Engineering Research Council Discovery Grant. The authors would like to thank Dr. Greg Evans, Dr. Yue Zhao and Dr. Christopher Lim for helpful comments and discussions. Special thanks to SOCAAR for providing the $SO_2$ analyzer.

https://doi.org/10.5194/acp-2020-983
Preprint. Discussion started: 12 October 2020


Atmospheric Chemistry and Physics Discussions

## Reference

Abbatt, J. P. D., Lee, A. K. Y., and Thornton, J. A.: Quantifying trace gas uptake to tropospheric aerosol: recent advances and remaining challenges, Chem. Soc. Rev., 41, 6555–6581, https://doi.org/10.1039/c2cs35052a, 2012.

Adams, J. W., Rodriguez, D., and Cox, R. A.: The uptake of $SO_2$ on Saharan dust: a flow tube study, Atmos. Chem. Phys., 5, 2643–2676, doi:10.5194/acp-5-2643-2005, 2005.

Andreae, M.O., Afchine, A., Albrecht, R., Holanda, B.A., Artaxo, P., Barbosa, H.M., Borrmann, S., Cecchini, M.A., Costa, A., Dollner, M. and Fütterer, D.: Aerosol characteristics and particle production in the upper troposphere over the Amazon Basin, Atmos. Chem. Phys., 18, 921–961, 2018.

Atkinson, R., and Arey, J.: Atmospheric degradation of volatile organic compounds, Chem. Rev., 103, 4605-4638, 2003.

Berndt, T., Richters, S., Kaethner, R., Voigtländer, J., Stratmann, F., Sipilä, M., Kulmala, M., and Herrmann, H.: Gas-phase ozonolysis of cycloalkenes: Formation of highly oxidized $RO_2$ radicals and their reactions with NO, $NO_2$, $SO_2$, and other $RO_2$ radicals, J. Phys. Chem. A, 119, 10336-10348, 10.1021/acs.jpca.5b07295, 2015.

Bianchi, F., Kurtén, T., Riva, M., Mohr, C., Rissanen, M. P., Roldin, P., Berndt, T., Crounse, J. D., Wennberg, P. O., Mentel, T. F., Wildt, J., Junninen, H., Jokinen, T., Kulmala, M., Worsnop, D. R., Thornton, J. A., Donahue, N., Kjaergaard, H. G., and Ehn, M.: Highly oxygenated organic molecules (HOM) from gas-phase autoxidation involving peroxy radicals: A key contributor to atmospheric aerosol, Chem. Rev., 119, 3472-3509, 10.1021/acs.chemrev.8 b00395, 2019.

Bonn, B., von Kuhlmann, R., and Lawrence, M. G.: High contribution of biogenic hydroperoxides to secondary organic aerosol formation, Geophys. Res. Lett., 31, L10108, https://doi.org/10.1029/2003GL019172, 2004.

Chen, Q., Farmer, D. K., Schneider, J., Zorn, S. R., Heald, C. L., Karl, T. G., Guenther, A., Allan, J. D., Robinson, N., Coe, H., Kimmel, J. R., Pauliquevis, T., Borrmann, S., Pöschl, U., Andreae, M. O., Artaxo, P., Jimenez, J. L., and Martin, S. T.: Mass spectral characterization of submicron biogenic organic particles in the Amazon Basin, Geophys. Res. Lett., 36, L20806, https://doi.org/10.1029/2009GL039880, 2009.

Chen, T., Chu, B., Ge, Y., Zhang, S., Ma, Q., He, H., and Li, S.-M.: Enhancement of aqueous sulfate formation by the coexistence of $NO_2$/$NH_3$ under high ionic strengths in aerosol water, Environ. Pollut., 252, 236-244, https://doi.org/10.1016/j.envpol.2019.05.119, 2019.

Cheng, Y., Su, H., Koop, T., Mikhailov, E., and Pöschl, U.: Size dependence of phase transitions in aerosol nanoparticles, Nat. Commun., 6, 5923, 10.1038/ncomms6923, 2015.

Cheng, Y. F., Zheng, G. J., Wei, C., Mu, Q., Zheng, B., Wang, Z. B., Gao, M., Zhang, Q., He, K. B., Carmichael, G., Pöschl, U., and Su, H.: Reactive nitrogen chemistry in aerosol water as a source of sulfate during haze events in China, Sci. Adv., 2, e1601530, https://doi.org/10.1126/ sciadv.1601530, 2016.

Ciobanu, V. G., Marcolli, C., Krieger, U. K., Weers, U., and Peter, T.: Liquid-liquid phase separation in mixed organic/inorganic aerosol particles, J. Phys. Chem. A, 113, 10966–10978, 2009.

Clegg, S. L., Brimblecombe, P., and Wexler, A. S.: Thermodynamic model of the system $H^+$–$NH_4^+$ –$Na^+$–$SO_4^{2-}$ –$NO_3^-$ –$Cl^-$–$H_2O$ at 298.15 K, J. Phys. Chem. A, 102, 2155–2171, https://doi.org/10.1021/jp973043j, 1998.

https://doi.org/10.5194/acp-2020-983
Preprint. Discussion started: 12 October 2020




571 Docherty, K. S., Wu, W., Lim, Y. B., and Ziemann, P. J.: Contributions of organic peroxides to
572 secondary aerosol formed from reactions of monoterpenes with $O_3$, Environ. Sci. Technol., 39,
573 4049-4059, 2005.
574 Dovrou, E., Rivera-Rios, J. C., Bates, K. H., and Keutsch, F. N.: Sulfate Formation via Cloud
575 Processing from Isoprene Hydroxyl Hydroperoxides (ISOPOOH), Environ. Sci. Technol., 53,
576 12476-12484, 10.1021/acs.est.9b04645, 2019.
577 Drozd, G. T., Woo, J. L., and McNeill, V. F.: Self-limited uptake of α-pinene oxide to acidic
578 aerosol: the effects of liquid-liquid phase separation and implications for the formation of
579 secondary organic aerosol and organosulfates from epoxides, Atmos. Chem. Phys., 13, 8255–
580 8263, doi:10.5194/acp-13-8255-2013, 2013.
581 Epstein, S. A., Blair, S. L., and Nizkorodov, S. A.: Direct photolysis of α-pinene ozonolysis
582 secondary organic aerosol: effect on particle mass and peroxide content, Environ. Sci. Technol.,
583 48, 11251-11258, 2014.
584 Fairlie, T. D., Jacob, D. J., Dibb, J. E., Alexander, B., Avery, M. A., van Donkelaar, A., and
585 Zhang, L.: Impact of mineral dust on nitrate, sulfate, and ozone in transpacific Asian pollution
586 plumes, Atmos. Chem. Phys., 10, 3999–4012, doi:10.5194/acp-10-3999-2010, 2010.
587 Freedman, M. A.: Phase separation in organic aerosol, Chem. Soc. Rev., 46, 7694–7705,
588 https://doi.org/10.1039/C6CS00783J, 2017.
589 Fu, H. B., Wang, X., Wu, H. B., Yin, Y., and Chen, J. M.: Heterogeneous uptake and oxidation
590 of $SO_2$ on iron oxides, J. Phys. Chem. C, 111, 6077–6085, 2007.
591 Gao, M., Carmichael, G. R., Wang, Y., Saide, P. E., Yu, M., Xin, J., Liu, Z., and Wang, Z.:
592 Modeling study of the 2010 regional haze event in the North China Plain, Atmos. Chem. Phys.,
593 16, 1673–1691, https://doi.org/10.5194/acp-16-1673-2016, 2016.
594 Gaston, C. J., Riedel, T. P., Zhang, Z., Gold, A., Surratt, J. D., and Thornton, J. A.: Reactive
595 uptake of an isoprene-derived epoxydiol to submicron aerosol particles, Environ. Sci. Technol.,
596 48, 11178-11186, 10.1021/es5034266, 2014.
597 Gen, M., Zhang, R., Huang, D. D., Li, Y., and Chan, C. K.: Heterogeneous SO2 Oxidation in
598 Sulfate Formation by Photolysis of Particulate Nitrate, Environ. Sci. Tech. Let., 6, 86–91,
599 https://doi.org/10.1021/acs.estlett.8b00681, 2019.
600 Griffiths, P. T., Badger, C. L., Cox, R. A., Folkers, M., Henk, H. H., and Mentel, T. F.: Reactive
601 uptake of $N_2O_5$ by aerosols containing dicarboxylic acids. Effect of particle phase, composition,
602 and nitrate content, J. Phys. Chem. A, 113, 5082-5090, 10.1021/jp8096814, 2009.
603 Gunz, D. W. and Hoffmann, M. R.: Atmospheric chemistry of peroxides: A review, Atmos.
604 Environ., 24A, 1601–1633, https://doi.org/10.1016/0960-1686(90)90496-A, 1990.
605 Guo, H., Weber, R. J., and Nenes, A.: High levels of ammonia do not raise fine particle pH
606 sufficiently to yield nitrogen oxide-dominated sulfate production, Sci. Rep., 7, 12109, 2017.
607 Hallquist, M., Wenger, J. C., Baltensperger, U., Rudich, Y., Simpson, D., Claeys, M., Dommen,
608 J., Donahue, N. M., George, C., Goldstein, A. H., Hamilton, J. F., Herrmann, H., Hoffmann, T.,
609 Iinuma, Y., Jang, M., Jenkin, M. E., Jimenez, J. L., Kiendler-Scharr, A., Maenhaut, W.,
610 McFiggans, G., Mentel, Th. F., Monod, A., Prévôt, A. S. H., Seinfeld, J. H., Surratt, J. D.,
611 Szmigielski, R., and Wildt, J.: The formation, properties and impact of secondary organic
612 aerosol: current and emerging issues, Atmos. Chem. Phys., 9, 5155–5236, https://doi.org/10.51
613 94/acp9-5155-2009, 2009.
614 Halperin, J., and Taube, H.: The transfer of oxygen atoms in oxidation—reduction reactions. IV.
615 The reaction of hydrogen peroxide with sulfite and thiosulfate, and of oxygen, manganese
616 dioxide and of permanganate with sulfite, J. Am. Chem. Soc., 74, 380-382, 1952.

https://doi.org/10.5194/acp-2020-983
Preprint. Discussion started: 12 October 2020


Atmospheric Chemistry and Physics Discussions

617 Hanson, D. R., Ravishankara, A. R., and Solomon, S.: Heterogeneous reactions in sulfuric acid
618 aerosols: A framework for model calculations, J. Geophys. Res., 99, 3615, https://doi.org/
619 10.1029/93JD02932, 1994.
620 Hartz, K. E. H., Rosenorn, T., Ferchak, S. R., Raymond, T. M., Bilde, M., Donahue, N. M., and
621 Pandis, S. N.: Cloud condensation nuclei activation of monoterpene and sesquiterpene
622 secondary organic aerosol, J. Geophys. Res.-Atmos., 110(D14), D14208, doi:10.1029/2004J
623 D005754, 2005.
624 He, L.-Y., Huang, X.-F., Xue, L., Hu, M., Lin, Y., Zheng, J., Zhang, R., and Zhang, Y.-H.:
625 Submicron aerosol analysis and organic source apportionment in an urban atmosphere
626 in Pearl River Delta of China using high-resolution aerosol mass spectrometry, J. Geophys. Res.-
627 Atmos., 116, D12304, https://doi.org/10.1029/2010JD014566, 2011.
628 Herrmann, H.: Kinetics of aqueous phase reactions relevant for atmospheric chemistry, Chem.
629 Rev., 103, 4691–4716, 2003.
630 Hildebrandt, L., Donahue, N. M., Pandis, S. N.: High formation of secondary organic aerosol
631 from the photo-oxidation of toluene, Atmos. Chem. Phys., 9, 2973–2986, https://doi.org
632 /10.5194/acp-9-2973-2009, 2009.
633 Huang, L., An, J., Koo, B., Yarwood, G., Yan, R., Wang, Y., Huang, C., and Li, L.: Sulfate
634 formation during heavy winter haze events and the potential contribution from heterogeneous
635 $SO_2 + NO_2$ reactions in the Yangtze River Delta region, China, Atmos. Chem. Phys., 19, 14311-
636 14328, 10.5194/acp-19-14311-2019, 2019.
637 Huang, L., Coddens, E. M., and Grassian, V. H.: Formation of organosulfur compounds from
638 aqueous phase reactions of S (IV) with methacrolein and methyl vinyl ketone in the presence of
639 transition metal ions, ACS Earth Space Chem., 3, 1749-1755, 2019.
640 Huang, L., Liu, T. and Grassian, V. H.: Radical-initiated formation of aromatic organosulfates
641 and sulfonates in the aqueous phase. Environ. Sci. Technol., 54, 11857–11864,
642 https://doi.org/10.1021/acs.est.0c05644, 2020.
643 Huang, R. J., Zhang, Y. L., Bozzetti, C., Ho, K. F., Cao, J. J., Han, Y. M., Daellenbach, K. R.,
644 Slowik, J. G., Platt, S. M., Canonaco, F., Zotter, P., Wolf, R., Pieber, S. M., Bruns, E. A., Crippa,
645 M., Ciarelli, G., Piazzalunga, A., Schwikowski, M., Abbaszade, G., Schnelle-Kreis, J.,
646 Zimmermann, R., An, Z., Szidat, S., Baltensperger, U., Haddad, I. E., and Prevot, A. S. H.: High
647 secondary aerosol contribution to particulate pollution during haze events in China, Nature, 514,
648 218–222, 2014.
649 Huang, R. J., He, Y., Duan, J., Li, Y., Chen, Q., Zheng, Y., Chen, Y., Hu, W., Lin, C., Ni, H.,
650 Dai, W., Cao, J., Wu, Y., Zhang, R., Xu, W., Ovadnevaite, J., Ceburnis, D., Hoffmann, T., and
651 O'Dowd, C. D.: Contrasting sources and processes of particulate species in haze days with low
652 and high relative humidity in wintertime Beijing, Atmos. Chem. Phys., 20, 9101-9114,
653 10.5194/acp-20-9101-2020, 2020.
654 Jang, M., and Kamens, R. M.: Atmospheric secondary aerosol formation by heterogeneous
655 reactions of aldehydes in the presence of a sulfuric acid aerosol catalyst, Environ. Sci. Technol.,
656 35, 4758-4766, 10.1021/es010790s, 2001.
657 Jimenez, J. L., Canagaratna, M. R., Donahue, N. M., Prevot, A. S. H., Zhang, Q., Kroll, J. H.,
658 DeCarlo, P. F., Allan, J. D., Coe, H., Ng, N. L., Aiken, A. C., Docherty, K. S., Ulbrich, I. M.,
659 Grieshop, A. P., Robinson, A. L., Duplissy, J., Smith, J. D., Wilson, K. R., Lanz, V. A., Hueglin,
660 C., Sun, Y. L., Tian, J., Laaksonen, A., Raatikainen, T., Rautiainen, J., Vaattovaara, P., Ehn, M.,
661 Kulmala, M., Tomlinson, J. M., Collins, D. R., Cubison, M. J., Dunlea, J., Huffman, J. A.,
662 Onasch, T. B., Alfarra, M. R., Williams, P. I., Bower, K., Kondo, Y., Schneider, J., Drewnick,

https://doi.org/10.5194/acp-2020-983
Preprint. Discussion started: 12 October 2020




F., Borrmann, S., Weimer, S., Demerjian, K., Salcedo, D., Cottrell, L., Griffin, R., Takami, A., Miyoshi, T., Hatakeyama, S., Shimono, A., Sun, J. Y., Zhang, Y. M., Dzepina, K., Kimmel, J. R., Sueper, D., Jayne, J. T., Herndon, S. C., Trimborn, A. M., Williams, L. R., Wood, E. C., Middlebrook, A. M., Kolb, C. E., Baltensperger, U., and Worsnop, D. R.: Evolution of organic aerosols in the atmosphere, Science, 326, 1525–1529, https://doi.org/10.1126/science.1180353, 2009.

Kautzman, K., Surratt, J., Chan, M., Chan, A., Hersey, S., Chhabra, P., Dalleska, N., Wennberg, P., Flagan, R., and Seinfeld, J.: Chemical composition of gas-and aerosol-phase products from the photooxidation of naphthalene, J. Phys. Chem. A, 114, 913-934, 2009.

Knipping, E. M., Lakin, M. J., Foster, K. L., Jungwirth, P., Tobias, D. J., Gerber, R. B., Dabdub, D., and Finlayson-Pitts, B. J.: Experiments and simulations of ion-enhanced interfacial chemistry on aqueous NaCl aerosols, Science, 288, 301, 10.1126/science.288.5464.301, 2000.

Krapf, M., El Haddad, I., Bruns, E. A., Molteni, U., Daellenbach, K. R., Prévôt, A. S., Baltensperger, U., and Dommen, J.: Labile peroxides in secondary organic aerosol, Chem, 1, 603-616, 2016.

Laskin, A., Gaspar, D. J., Wang, W., Hunt, S. W., Cowin, J. P., Colson, S. D., and Finlayson-Pitts, B. J.: Reactions at interfaces as a source of sulfate formation in sea-salt particles, Science, 301, 340, 10.1126/science.1085374, 2003.

Leng, C. B., Roberts, J. E., Zeng, G., Zhang, Y. H., and Liu, Y.: Effects of temperature, pH, and ionic strength on the Henry's law constant of triethylamine, Geophys. Res. Lett., 42, 3569-3575, 10.1002/2015gl063840, 2015.

Li, G., Bei, N., Cao, J., Huang, R., Wu, J., Feng, T., Wang, Y., Liu, S., Zhang, Q., Tie, X., and Molina, L. T.: A possible pathway for rapid growth of sulfate during haze days in China, Atmos. Chem. Phys., 17, 3301–3316, https://doi.org/10.5194/acp17-3301-2017, 2017.

Li, J., Zhang, Y., Cao, F., Zhang, W., Fan, M., Lee, X., Michalski, G.: Stable sulfur isotopes revealed a major role of transition-metal-ion catalyzed $SO_2$ oxidation in haze episodes, doi:10.1021/acs.est.9b07150, 2020.

Lind, J. A., Lazrus, A. L., and Kok, G. L.: Aqueous phase oxidation of sulfur (IV) by hydrogen peroxide, methylhydroperoxide, and peroxyacetic acid, J. Geophys. Res. Atmos., 92, 4171-4177, 1987.

Liu, C., Chen, T., Liu, Y., Liu, J., He, H., Zhang, P.: Enhancement of secondary organic aerosol formation and its oxidation state by $SO_2$ during photooxidation of 2-methoxyphenol, Atmos. Chem. Phys., 19, 2687-2700, 2019.

Liu, L., Bei, N., Wu, J., Liu, S., Zhou, J., Li, X., Yang, Q., Feng, T., Cao, J., Tie, X. and Li, G.: Effects of stabilized Criegee intermediates (sCIs) on sulfate formation: a sensitivity analysis during summertime in Beijing–Tianjin–Hebei (BTH), China, Atmos. Chem. Phys., 19, 13341-13354, 2019.

Liu, T., Clegg, S. L. and Abbatt, J. P. D.: Fast oxidation of sulfur dioxide by hydrogen peroxide in deliquesced aerosol particles, Proc. Natl. Acad. Sci. U. S. A., 117, 1354–1359, 2020.

Liu, Y., Liggio, J., Staebler, R., and Li, S. M.: Reactive uptake of ammonia to secondary organic aerosols: kinetics of organonitrogen formation, Atmos. Chem. Phys., 15, 13569–13584, doi:10.5194/acp-15-13569-2015, 2015.

Maaß, F., Elias, H., and Wannowius, K. J.: Kinetics of the oxidation of hydrogen sulfite by hydrogen peroxide in aqueous solution: ionic strength effects and temperature dependence, Atmos. Environ., 33, 4413-4419, https://doi.org/10.1016/S1352-2310(99)00212-5, 1999.

https://doi.org/10.5194/acp-2020-983
Preprint. Discussion started: 12 October 2020




708 Mauldin, R. L., Berndt, T., Sipilä, M., Paasonen, P., Petäjä, T., Kim, S., Kurtén, T., Stratmann,
709 F., Kerminen, V. M., and Kulmala, M.: A new atmospherically relevant oxidant of sulphur
710 dioxide, Nature, 488, 193–196, https://doi.org/10.1038/nature11278, 2012.
711 Mekic, M., Loisel, G., Zhou, W., Jiang, B., Vione, D., and Gligorovski, S.: Ionic-strength effects
712 on the reactive uptake of ozone on aqueous pyruvic acid: Implications for air–sea ozone
713 deposition, Environ. Sci. Technol., 52, 12306-12315, 10.1021/acs.est.8b03196, 2018.
714 Mekic, M., Zeng, J., Zhou, W., Loisel, G., Jin, B., Li, X., Vione, D., and Gligorovski, S.: Ionic
715 strength effect on photochemistry of fluorene and dimethylsulfoxide at the air–sea interface:
716 Alternative formation pathway of organic sulfur compounds in a marine atmosphere, ACS Earth
717 Space Chem., 4, 1029-1038, 10.1021/acsearthspacechem.0c00059, 2020.
718 Mishra, H., Enami, S., Nielsen, R. J., Hoffmann, M. R., Goddard, W. A., and Colussi, A. J.:
719 Anions dramatically enhance proton transfer through aqueous interfaces, Proc. Natl. Acad. Sci.
720 U. S. A., 109, 10228-10232, 2012.
721 Ng, N., Kroll, J., Chan, A., Chhabra, P., Flagan, R., and Seinfeld, J.: Secondary organic aerosol
722 formation from m-xylene, toluene, and benzene, Atmos. Chem. Phys., 7, 3909–3922,
723 http://www.atmos-chem-phys.net/7/3909/2007, 2007.
724 Ng, N. L., Kwan, A. J., Surratt, J. D., Chan, A. W. H., Chhabra, P. S., Sorooshian, A., Pye, H. O.
725 T., Crounse, J. D., Wennberg, P. O., Flagan, R. C., and Seinfeld, J. H.: Secondary organic
726 aerosol (SOA) formation from reaction of isoprene with nitrate radicals ($NO_3$), Atmos. Chem.
727 Phys., 8, 4117–4140, http://www.atmos-chem-phys.net/8/4117/2008/, 2008.
728 O'Brien, R. E., Wang, B., Kelly, S. T., Lundt, N., You, Y., Bertram, A. K., Leone, S. R., Laskin,
729 A., and Gilles, M. K.: Liquid–liquid phase separation in aerosol particles: Imaging at the
730 nanometer scale, Environ. Sci. Technol., 49, 4995-5002, 10.1021/acs.est.5b00062, 2015.
731 Pankow, J. F. and Asher, W. E.: SIMPOL.1: a simple group contribution method for predicting
732 vapor pressures and enthalpies of vaporization of multifunctional organic compounds, Atmos.
733 Chem. Phys., 8, 2773–2796, http://www.atmos-chem-phys.net/8/2773/2008/, 2008.
734 Qiu, J., Liang, Z., Tonokura, K., Colussi, A. J., and Enami, S.: Stability of monoterpene-derived
735 α-hydroxyalkyl-hydroperoxides in aqueous qrganic media – relevance to the fate of
736 hydroperoxides in aerosol particle phases, Environ. Sci. Technol., 10.1021/acs.est.9b07497,
737 2020.
738 Rodríguez-Sevilla, J., Álvarez, M., Limiñana, G., Díaz, M. C.: Dilute $SO_2$ absorption equilibria
739 in aqueous HCl and NaCl solutions at 298.15 K, J. Chem. Eng. Data, 47, 1339-1345, 2002.
740 Ruiz-Lopez, M.F., Francisco, J.S., Martins-Costa, M.T. and Anglada, J.M.: Molecular reactions
741 at aqueous interfaces. Nat. Rev. Chem., 1-17, 2020.
742 Seinfeld, J. H., and Pandis, S. N.: Atmospheric chemistry and physics: from air pollution to
743 climate change, John Wiley & Sons, 2012.
744 Sha, T., Ma, X., Jia, H., Tian, R., Chang, Y., Cao, F., and Zhang, Y.: Aerosol chemical
745 component: Simulations with WRF-Chem and comparison with observations in Nanjing, Atmos.
746 Environ., 218, 116982, https://doi.org/10.1016/j.atmosenv.2019.116982, 2019.
747 Shang, J., Li, J., Zhu, T.: Heterogeneous reaction of $SO_2$ on $TiO_2$ particles. Sci.
748 China Chem., 53, 2637–2643, 2010.
749 Shi, Q., Davidovits, P., Jayne, J. T., Worsnop, D. R., and Kolb, C. E.: Uptake of gas-phase
750 ammonia. 1. Uptake by aqueous surfaces as a function of pH, J. Phys. Chem. A, 103, 8812-8823,
751 10.1021/jp991696p, 1999.
752 Song, M., Marcolli, C., Krieger, U. K., Zuend, A., and Peter, T.: Liquid–liquid phase separation

https://doi.org/10.5194/acp-2020-983
Preprint. Discussion started: 12 October 2020


Atmospheric Chemistry and Physics Discussions

753 in aerosol particles: dependence on O:C, organic functionalities, and compositional complexity,
754 Geophys. Res. Lett., 39, L19801, doi:10.1029/2012GL052807, 2012.
755 Song, S., Gao, M., Xu, W., Shao, J., Shi, G., Wang, S., Wang, Y., Sun, Y., and McElroy, M. B.:
756 Fine-particle pH for Beijing winter haze as inferred from different thermodynamic equilibrium
757 models, Atmos. Chem. Phys., 18, 7423–7438, https://doi.org/10.5194/acp-18-7423-2018, 2018.
758 Song, S., Gao, M., Xu, W., Sun, Y., Worsnop, D. R., Jayne, J. T., Zhang, Y., Zhu, L., Li, M.,
759 Zhou, Z., Cheng, C., Lv, Y., Wang, Y., Peng, W., Xu, X., Lin, N., Wang, Y., Wang, S., Munger,
760 J. W., Jacob, D. J., and McElroy, M. B.: Possible heterogeneous chemistry of hydroxy
761 methanesulfonate (HMS) in northern China winter haze, Atmos. Chem. Phys., 19, 1357–1371,
762 https://doi.org/10.5194/acp-19-1357-2019, 2019.
763 Su, H., Cheng, Y., and Poschl, U.: New multiphase chemical processes influencing atmospheric
764 aerosols, air quality, and climate in the anthropocene, Acc. Chem. Res., e1601530-2983,
765 https://doi.org/10.1021/acs.accounts.0c00246, 2020.
766 Sun, Y., Wang, Z., Fu, P., Jiang, Q., Yang, T., Li, J., and Ge, X.: The impact of relative humidity
767 on aerosol composition and evolution processes during wintertime in Beijing, China, Atmos.
768 Environ., 77, 927-934, 2013.
769 Surratt, J. D., Murphy, S. M., Kroll, J. H., Ng, N. L., Hildebrandt, L., Sorooshian, A.,
770 Szmigielski, R., Vermeylen, R., Maenhaut, W., and Claeys, M.: Chemical composition of
771 secondary organic aerosol formed from the photooxidation of isoprene, J. Phys. Chem. A, 110,
772 9665-9690, 2006.
773 Thornton, J. A., Braban, C. F., and Abbatt, J. P. D.: $N_2O_5$ hydrolysis on sub-micron organic
774 aerosols: the effect of relative humidity, particle phase, and particle size, Phys. Chem. Chem
775 Phys., 5, 4593–4603, https://doi.org/10.1039/B307498F, 2003.
776 Tie, X., Brasseur, G., Emmons, L., Horowitz, I., and Kinnison, D.: Effects of aerosols on
777 tropospheric oxidants: a global model study, J. Geophys. Res. Atmos., 106, 22931–22964, 2001.
778 Usher, C. R., Al-Hosney, H., Carlos-Cuellar, S., and Grassian,V. H.: A laboratory study of the
779 heterogeneous uptake and oxidation of sulfur dioxide on mineral dust particles, J. Geophys.
780 Res., 107, 4713, doi:10.1029/2002JD002051, 2002.
781 Varutbangkul, V., Brechtel, F. J., Bahreini, R., Ng, N. L., Keywood, M. D., Kroll, J. H., Flagan,
782 R. C., Seinfeld, J. H., Lee, A., and Goldstein, A. H.: Hygroscopicity of secondary organic
783 aerosols formed by oxidation of cycloalkenes, monoterpenes, sesquiterpenes, and related
784 compounds, Atmos. Chem. Phys., 6, 2367–2388, http://www.atmos-chem-phys.net/6/23
785 67/2006/, 2006.
786 Veghte, D. P., Altaf, M. B., and Freedman, M. A.: Size dependence of the structure of organic
787 aerosol, J. Am. Chem. Soc.,135, 16046–16049, 2013.
788 Wang, G., Zhang, R., Gomez, M. E., Yang, L., Zamora, M. L., Hu, M., Lin, Y., Peng, J., Guo, S.,
789 and Meng, J.: Persistent sulfate formation from London Fog to Chinese haze, Proc. Natl. Acad.
790 Sci. U. S. A., 113, 13630-13635, 2016.
791 Wang, S., Ye, J., Soong, R., Wu, B., Yu, L., Simpson, A. J., and Chan, A. W. H.: Relationship
792 between chemical composition and oxidative potential of secondary organic aerosol from
793 polycyclic aromatic hydrocarbons, Atmos. Chem. Phys., 18, 3987-4003, 2018.
794 Wang, S., Zhou, S., Tao, Y., Tsui, W. G., Ye, J., Yu, J. Z., Murphy, J. G., McNeill, V. F.,
795 Abbatt, J. P. D., and Chan, A. W. H.: Organic peroxides and sulfur dioxide in aerosol: Source of
796 particulate sulfate, Environ. Sci. Technol., 53, 10695-10704, 10.1021/acs.est.9b02591, 2019.
797 Wang, X.; Gemayel, R.; Hayeck, N.; Perrier, S.; Charbonnel, N.; Xu, C.; Chen, H.; Zhu, C.;
798 Zhang, L.; Wang, L.; Nizkorodov, S. A.; Wang, X.; Wang, Z.; Wang, T.; Mellouki, A.; Riva, M.;

https://doi.org/10.5194/acp-2020-983
Preprint. Discussion started: 12 October 2020




799 Chen, J.; George, C. Atmospheric photosensitization: A new pathway for sulfate formation,
800 Environ. Sci. Technol., 54, 3114-3120, 2020.
801 Wang, Y., Zhang, Q., Jiang, J., Zhou, W., Wang, B., He, K., Duan, F., Zhang, Q., Philip, S., and
802 Xie, Y.: Enhanced sulfate formation during China's severe winter haze episode in January 2013
803 missing from current models, J. Geophys. Res. Atmos., 119, 10425–10440, https://doi.org/10.10
804 02/2013JD021426, 2014.
805 Wei, H., Vejerano, E. P., Leng, W., Huang, Q., Willner, M. R., Marr, L. C., and Vikesland, P. J.:
806 Aerosol microdroplets exhibit a stable pH gradient, Proc. Natl. Acad. Sci. U. S. A., 115, 7272,
807 10.1073/pnas.1720488115, 2018.
808 Xu, L., Guo, H., Boyd, C. M., Klein, M., Bougiatioti, A., Cerully, K. M., Hite, J. R., Isaacman-
809 VanWertz, G., Kreisberg, N. M., and Knote, C.: Effects of anthropogenic emissions on aerosol
810 formation from isoprene and monoterpenes in the southeastern United States, Proc. Natl. Acad.
811 Sci. U. S. A., 112, 37-42, 2015.
812 Yang, Y., Wang, H., Smith, S. J., Easter, R., Ma, P.-L., Qian, Y., Yu, H., Li, C., and Rasch, P. J.:
813 Global source attribution of sulfate concentration and direct and indirect radiative forcing,
814 Atmos. Chem. Phys., 17, 8903–8922, https://doi.org/10.5194/acp17-8903-2017, 2017.
815 Yao, M., Zhao, Y., Hu, M., Huang, D., Wang, Y.C., Yu, J. Z., and Yan, N.: Multiphase reactions
816 between secondary organic aerosol and sulfur dioxide: kinetics and contributions to sulfate
817 formation and aerosol aging, Environ. Sci. Tech. Let. 6, 768-774, 10.1021/acs.est
818 lett.9b00657, 2019.
819 Ye, J., Gordon, C. A., and Chan, A. W. H: Enhancement in secondary organic aerosol formation
820 in the presence of preexisting organic particle, Environ. Sci. Technol., 50, 3572-3579, 2016.
821 Ye, J., Abbatt, J. P. D., and Chan, A. W. H.: Novel pathway of $SO_2$ oxidation in the atmosphere:
822 reactions with monoterpene ozonolysis intermediates and secondary organic aerosol, Atmos.
823 Chem. Phys., 18, 5549–5565, https://doi.org/10.5194/acp18-5549-2018, 2018.
824 Yee, L. D., Isaacman-VanWertz, G., Wernis, R. A., Kreisberg, N. M., Glasius, M., Riva, M.,
825 Surratt, J. D., de Sá, S. S., Martin, S. T., Alexander, M. L., Palm, B. B., Hu, W., Campuzano-
826 Jost, P., Day, D. A., Jimenez, J. L., Liu, Y., Misztal, P. K., Artaxo, P., Viegas, J., Manzi, A., de
827 Souza, R. A. F., Edgerton, E. S., Baumann, K., and Goldstein, A. H.: Natural and
828 anthropogenically influenced isoprene oxidation in southeastern United States and central
829 Amazon, Environ. Sci. Technol., 54, 5980-5991, 10.1021/acs.est.0c00805, 2020.
830 You, Y., Renbaum-Wolff, L., Bertram, A. K: Liquid-liquid phase separation in particles
831 containing organics mixed with ammonium sulfate, ammonium bisulfate, ammonium nitrate or
832 sodium chloride, Atmos. Chem. Phys., 13, 11723–11734, https://doi.org/10.5194/acp
833 -13-11723-2013, 2013.
834 You, Y., Smith, M. L., Song, M., Martin, S. T., and Bertram, A. K.: Liquid–liquid phase
835 separation in atmospherically relevant particles consisting of organic species and inorganic salts,
836 Int. Rev. Phys. Chem., 33, 43–77, doi:10.1080/0144235X.2014.890786, 2014.
837 Zhang, S., Xing, J., Sarwar, G., Ge, Y., He, H., Duan, F., Zhao, Y., He, K., Zhu, L. and Chu, B.:
838 Parameterization of heterogeneous reaction of $SO_2$ to sulfate on dust with coexistence of $NH_3$
839 and $NO_2$ under different humidity conditions, Atmos. Environ., 208, 133-140, 2019.
840 Zhao, Y., Liu, Y., Ma, J., Ma, Q., and He, H.: Heterogeneous reaction of $SO_2$ with soot: The
841 roles of relative humidity and surface composition of soot in surface sulfate formation, Atmos.
842 Environ., 152, 465-476, 2017.
843 Zheng, B., Zhang, Q., Zhang, Y., He, K. B., Wang, K., Zheng, G. J., Duan, F. K., Ma, Y. L., and
844 Kimoto, T.: Heterogeneous chemistry: a mechanism missing in current models to explain

https://doi.org/10.5194/acp-2020-983
Preprint. Discussion started: 12 October 2020


Atmospheric Chemistry and Physics Discussions

secondary inorganic aerosol formation during the January 2013 haze episode in North China, Atmos. Chem. Phys., 15, 2031–2049, doi:10.5194/acp-15-2031-2015, 2015.
Zheng, G. J., Duan, F. K., Su, H., Ma, Y. L., Cheng, Y., Zheng, B., Zhang, Q., Huang, T., Kimoto, T., Chang, D., Pöschl, U., Cheng, Y. F., and He, K. B.: Exploring the severe winter haze in Beijing: the impact of synoptic weather, regional transport and heterogeneous reactions, Atmos. Chem. Phys., 15, 2969–2983, doi:10.5194/acp-15-2969-2015, 2015.

https://doi.org/10.5194/acp-2020-983
Preprint. Discussion started: 12 October 2020


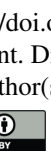

Atmospheric Chemistry and Physics Discussions

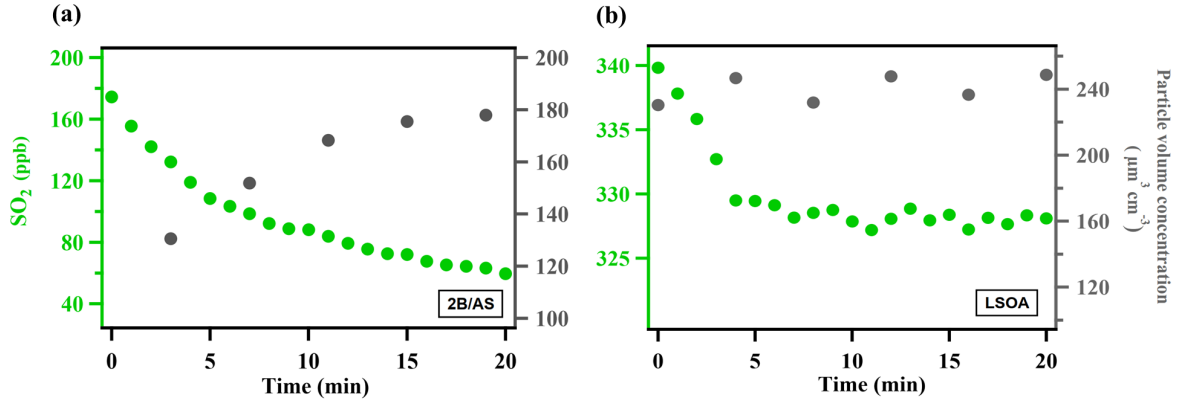


874

875 **Figure 1.** Typical evolution of the species monitored during $\gamma_{SO2}$ measurement for (a)
876 ammonium sulfate mixed with 2-butanone organic peroxide (2B/AS, Expt. 16) and (b) limonene
877 SOA (LSOA, Expt. 27). Particle volume concentrations measured by SMPS have been corrected
878 for wall loss assuming a pseudo first-order loss rate (Ye et al., 2016). $\gamma_{SO2}$ was calculated for the
879 initial portion of the decay (first 7 minutes).

880

881

882

883

884

885

https://doi.org/10.5194/acp-2020-983
Preprint. Discussion started: 12 October 2020


Atmospheric Chemistry and Physics Discussions

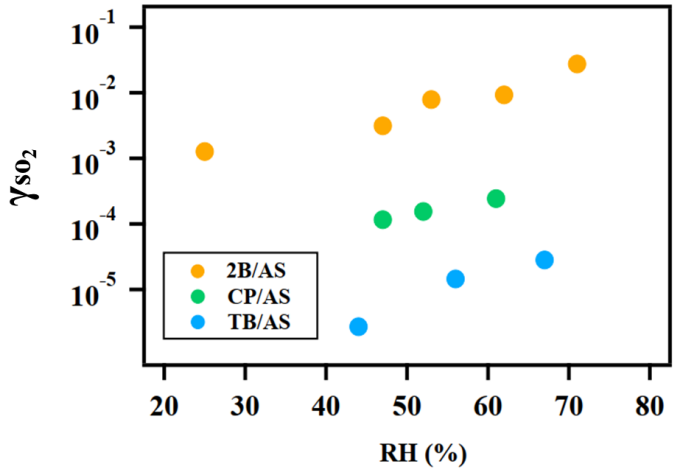


886

887 **Figure 2.** Exponential relationship between $\gamma_{SO2}$ and RH for ammonium sulfate aerosol

888 containing 2-butanone peroxide (2B), cumene hydroperoxide (CP), tert-butyl hydroperoxide

889 (TB).

890

891

892

893

894

895

896

897

https://doi.org/10.5194/acp-2020-983
Preprint. Discussion started: 12 October 2020


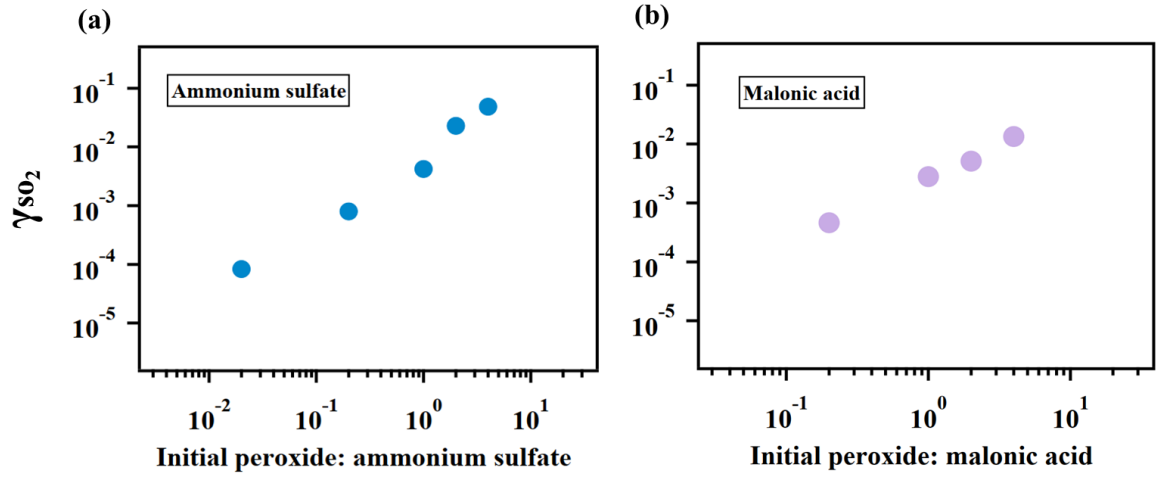


**Figure 3.** Relationship between $\gamma_{SO2}$ and particulate peroxide content. $\gamma_{SO2}$ for ammonium sulfate (a) and malonic acid aerosol (b) containing different amount of 2-butanone peroxide are shown here. The observed dependence of $\gamma_{SO2}$ on the amount of peroxide injected are linear since the slopes of the relationship are both nearly 1 in (a) and (b).

https://doi.org/10.5194/acp-2020-983
Preprint. Discussion started: 12 October 2020


Atmospheric Chemistry and Physics Discussions

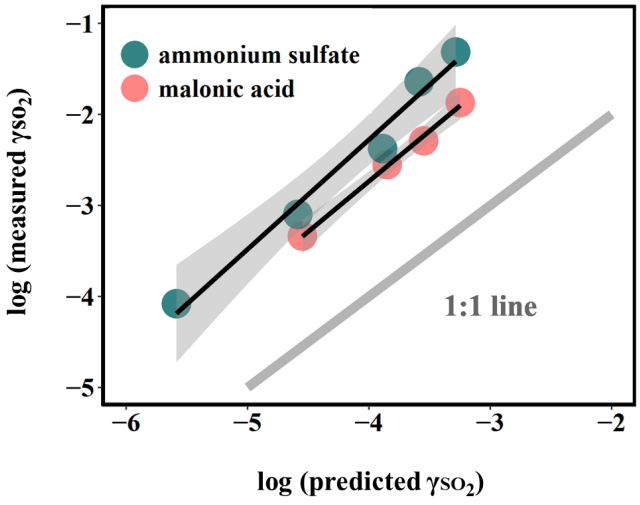


907

908 **Figure 4.** Relationship between measured $\gamma_{SO2}$ and $\gamma_{SO2}$ predicted by Eqn. 4. The large deviation
909 from the 1:1 line, which represents the difference between the measured uptake coefficient and
910 predicted values based on kinetics in the dilute aqueous phase, indicates that aerosol reactive
911 uptake is significantly faster than reactions in dilute aqueous phase. This enhancement is likely
912 driven in part by high ionic strengths, as the difference between measured $\gamma_{SO2}$ and predicted $\gamma_{SO2}$
913 are consistently higher for organic peroxide containing ammonium sulfate (high ionic strength)
914 than for that mixed with malonic acid (lower ionic strength).

915

916

917

918

919

https://doi.org/10.5194/acp-2020-983
Preprint. Discussion started: 12 October 2020


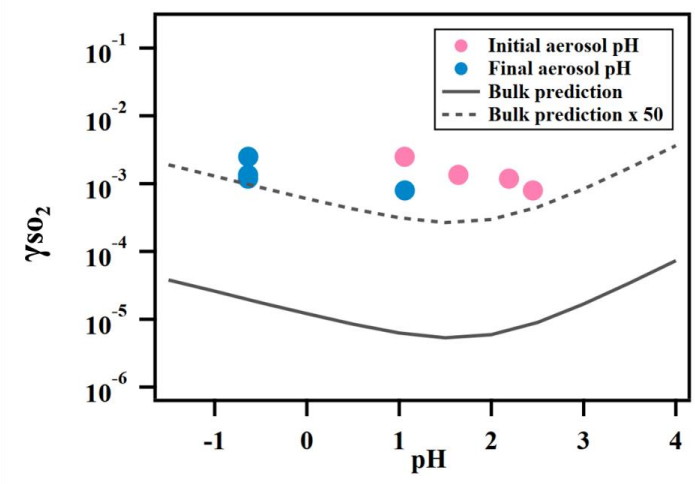


**Figure 5.** Relationship between $\gamma_{SO2}$ and aerosol phase pH for ammonium sulfate aerosol containing 2-butanone peroxide.

https://doi.org/10.5194/acp-2020-983
Preprint. Discussion started: 12 October 2020


Atmospheric Chemistry and Physics Discussions

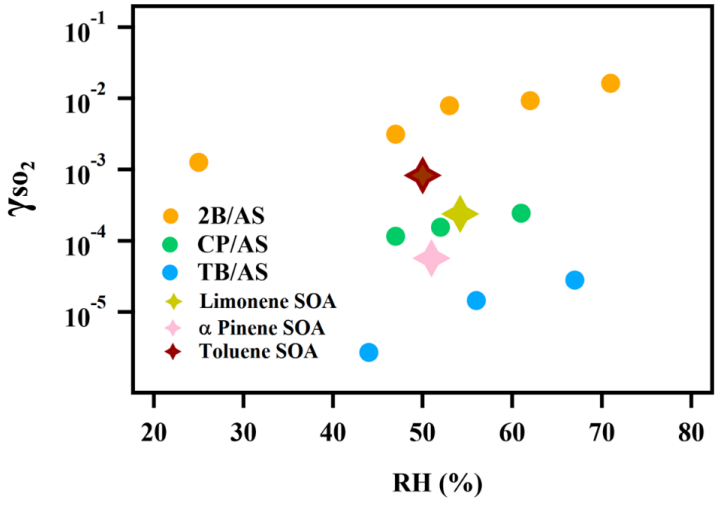


931

932 **Figure 6.** $\gamma_{SO2}$ measured for different types of organic aerosol. The reactive uptake coefficient of

933 $SO_2$ onto SOA are on the order of $10^{-4}$.

934

935

936

937

938

939

940

941

942

https://doi.org/10.5194/acp-2020-983
Preprint. Discussion started: 12 October 2020


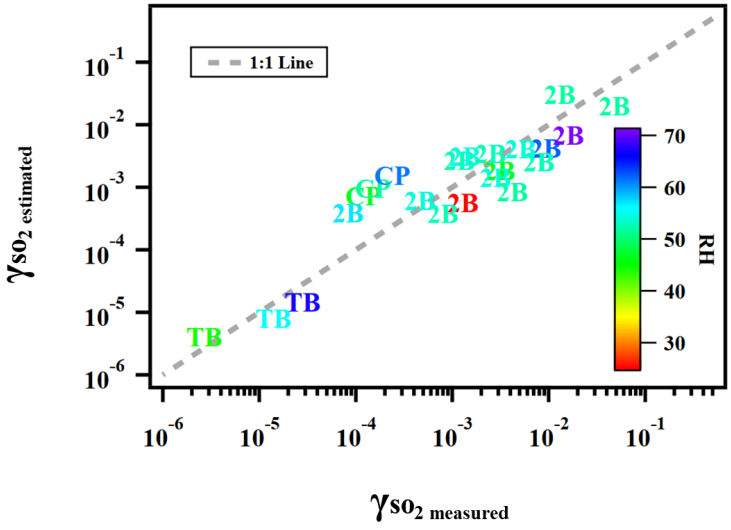


**Figure 7.** Predicted $\gamma_{SO2}$ using Equation (8) versus measured $\gamma_{SO2}$ for ammonium sulfate or malonic acid aerosol containing 2-butanone peroxide (2B), cumene hydroperoxide (CP), tert-butyl hydroperoxide (TB) under different experimental conditions.